This is a preproof accepted article for *Animal Nutriomics*
This version may be subject to change during the production process
DOI: 10.1017/anr.2025.10008

Zinc toxicity induces intestinal cell death via inhibiting NAD^+ synthesis in mice and IPEC-J2 cells

Lingjun Chen[1], Feifei Huang[1], Leilei Zhu[1], Xin Tian[1], Mohan Zhou[1], Jie Feng[1]*

Key Laboratory of Animal Nutrition & Feed Sciences of Zhejiang Province, College of Animal Science, Zhejiang University, Hangzhou 310058, China

***Corresponding author:** Jie Feng, email: fengj@zju.edu.cn

Abstract

Excessive zinc (Zn) intake can lead to Zn toxicity, causing adverse effects in gastrointestinal system. To date, there remains no definitive consensus on the mechanisms by which Zn overload induces cell death and intestinal injury. This study was to assess the toxicity mechanism of Zn overload in intestine, with a particular concentrate on oxidative stress and energy metabolism. We first explore the effects of short- and long-term Zn imbalances on intestinal health in mice. We found Zn imbalances resulted in oxidative damage, and impaired α-KGDH activity, which collectively contributed to a detrimental impact on the integrity of the intestinal barrier in mice. We next determined the dynamics of oxidative stress and energy metabolism in Zn overload treatment IPEC-J2 cells. Excessive Zn activated ROS overproduction and the PKC-NOX oxidative stress pathway. Moreover, the increase of mitochondrial Zn^{2+} caused mitochondrial ROS accumulation and influenced the expressions of α-KGDH and IDH, two pivotal rate-limiting enzymes in TCA cycle. Zn overload also significantly inhibited the expressions of key NAD^+ synthesis enzymes, namely NMNAT1 and NAMPT, leading to a notable decline of NAD^+ and ATP. Furthermore, rescue

experiments showed supplementation of NAD^+ or boosting NAD^+ synthesis, but not antioxidants addition, could rescue Zn toxicity. The collective findings suggest NAD^+ reduction is the primary factor contributing to intestinal Zn toxicity, although ROS also plays a role. This indicates that the modulation of NAD^+ synthesis may prove an effective strategy for the minimization or elimination of Zn toxicity.

Keywords: Zn toxicity, intestine, oxidative stress, energy metabolism, NAD^+

1 Introduction

Zinc (Zn) is an indispensable trace element for both human and animal organisms, constituting a vital component for the activation of over 300 enzymes within the body. Zn deficiency may result in growth retardation, hypogonadism, diarrhea, or enteropathic dermatitis [1]. In order to fulfill the physiological requirements of Zn, additional Zn is frequently incorporated into feed or nutritional supplements. Nevertheless, whether within the domain of public health or livestock husbandry, the levels of Zn supplementation tend to surpass the stipulated maximum tolerable intake levels for both humans and animals [2; 3]. This overconsumption of Zn may lead to a range of adverse effects, such as compromised immune capacity, impaired growth or sexual maturation, and augmented deposition of visceral fat [4-6].

Currently, the research on the mechanism of Zn toxicity has mainly focused on the nervous system, with limited and insufficient research on intestinal injury. Many studies proposed that oxidative stress may be a primary factor in cell death induced by Zn toxicity. Excessive Zn can generate cytotoxic reactive oxygen species (ROS) by activating nicotinamide adenine dinucleotide phosphate (NADPH) oxidase (NOX) [7; 8]. Consequently, this cascade of events triggers the activation of poly (ADP-ribose) polymerase (PARP) -1, leading to the release of the apoptosis-inducing factor (AIF), thereby inciting cellular apoptosis [9-12]. It was proposed several years ago that abnormal elevation of intracellular Zn can cause dysfunction of energy metabolism [13]. Excessive Zn can inhibit the activity of alpha-ketoglutarate dehydrogenase (α-KGDH) and isocitrate dehydrogenase (IDH) in the

tricarboxylic acid (TCA) cycle, severely impairing mitochondrial function and resulting in a reduction in intracellular ATP levels [14; 15].

The intestine, especially the jejunum, is the major location for Zn absorption and is highly susceptible to damage in the event of excessive Zn intake[16] [17]. The intestinal integrity is essential for the health and survival of animals. Damage to the intestinal barrier increases the penetration of pathogens and poisonous substances, leading to intestinal infections as well as poor health and performance in humans and animals. Our preliminary research findings indicated that, during Zn overload induced cell death in porcine small intestine epithelial cell line (IPEC-J2 cells), a sustained and significant decline in ATP levels was observed, while glutathione (GSH) levels remained constant in the later stages [18]. Based on these observations, we speculated that energy metabolism impairment may be a more prominent factor in Zn-induced intestinal cytotoxicity than oxidative damage. However, there is limited research on Zn overload-induced intestinal energy metabolism damage, and further investigation is required to explore the relationship between oxidative stress and energy metabolism impairment in the context of cell death induced by Zn cytotoxicity.

In this study, firstly, C57BL/6 mice were used as an *in vivo* model to investigate the effects of both long-term and short-term Zn overload on intestinal health. Then, IPEC-J2 cells were employed as an *in vitro* model to scrutinize the temporal dynamics of oxidative damage and energy metabolism impairment during Zn toxicity. Furthermore, a comprehensive inquiry was undertaken through the implementation of energy metabolism substrate compensation or the promotion of key enzymes in IPEC-J2 cells to discern whether energy metabolism inhibition predominates in the context of Zn overload-induced intestinal injury. The findings corroborate the hypothesis that the reduction of nicotinamide adenine dinucleotide (NAD^+) is a crucial determinant in Zn overload-induced intestinal toxicity.

2 Materials and Methods

2.1 Animal experiments

This work has received approval for research ethics from Animal Ethics Committee of Zhejiang University and a proof of approval is available upon request (Approval NO. ZJU20240808). Sixty-four male C57BL/6 mice (three weeks old), were randomly housed in

stainless steel cages (8 per cage) under controlled conditions (12-hour light/dark cycle, 20 ± 3°C), with free access to water and diets. As shown in Figure 1A, mice were fed modified zinc (Zn) diets for four weeks (short-term intervention) or eight weeks (long-term intervention). The zinc dosage in the feed refers to our previous study[19], included: low-Zn (no extra additional Zn), control-Zn (30 mg/kg Zn), high-Zn (150 mg/kg Zn), and excess-Zn (600 mg/kg Zn). Zn diets were formulated by SLAC Experimental Animals LLC. Following an 8-hour fast at the end of the experiment, mice were euthanized with cervical dislocation. Intestine samples were collected and stored at -80°C for analysis.

2.2 Cell culture

IPEC-J2 cells were cultured in DMEM/F12 medium supplemented with 10% FBS and 1% penicillin-streptomycin at 37°C and 5% CO_2-humidified incubator. Cells were seeded in 96-well plates for the viability assay and ATP level measurement, and in 6-well plates for other assays. Following treatment with 150 μM $ZnSO_4$ (Sigma Aldrich, USA), cell samples were collected at 1, 2, 3 and 4 h time points.

To investigate the effects of altered NAD^+ biosynthesis on Zn overload-induced harmful effects, the cells were treated with 150 μM $ZnSO_4$ in the presence or absence of NAMPT promoter NAT (2.5, 5 and 10 μmol/L, pretreated for 24 h), or transfected with overexpression plasmids NAMPT (pretreated for 24 h, NCBI Reference Sequence: NM_001031793.2) or NMNAT1 (pretreated for 24 h, NCBI Reference Sequence: XM_021095304.1).

2.3 Oxidative stress

The levels of malondialdehyde (MDA), total antioxidant capability (T-AOC) and nitric oxide (NO), as well as the activities of GSH and total superoxide dismutase (T-SOD), were assessed using specific commercial assay kits (Nanjing Jiancheng Bioengineering Institute, China). Sample analysis was performed in accordance with the manufacturer's instructions.

Measurement of jejunum ROS

Freshly prepared frozen jejunum sections were thawed for 2 hours at 37°C and then incubated with 2 μM dihydroethidium (DHE; Sigma Aldrich, USA) in PBS for 30 minutes at 37°C. Subsequently, counter-staining with DAPI was conducted, and images were captured using a fluorescent microscope (Leica, Germany) in two channels: Ex/Em=518/616 nm and

Ex/Em=360/460 nm.

Measurement of cell mitochondrial ROS

Zn-treated cells were collected using Accutase (Sigma Aldrich, US), thoroughly washed, and subsequently incubated in 500 μl of Hanks balanced salt solution (HBSS, Gibco) containing 5 μM MitoSOX Red (M36008, Invitrogen) for a duration of 10 minutes. After this incubation period, the assessment of mitochondrial ROS was carried out using a flow cytometer (FACSCalibur, BD Biosciences).

2.4 Western blotting

The total proteins of jejunum samples and IPEC-J2 cells were homogenized using subcellular structure membrane protein and cytoplasmic protein extraction kit (Boster Biological Technology, China) and RIPA lysis buffer (Beyotime, Shanghai, China) with 1% PMSF (Beyotime, Shanghai, China), respectively. Total protein content was quantified using the BCA protein assay kit (KeyGen Biotech, Nanjing, China). The extracted proteins were loaded onto a 12.5% SDS gel and subsequently transferred to a PVDF membrane. Then, the membranes were subjected to a 2-hour blocking step using a 5% fat-free milk solution. After blocking, membranes were probed with primary antibodies (Supplementary Table S1) overnight at 4°C, followed by HRP-conjugated secondary antibodies (1:5000 dilution). Chemiluminescence signals were detected using a LAS-4000CCD exposure system (Fujifilm). Band intensities were quantified using Image Lab™ software (Bio-Rad) with β-actin as the loading control. Background-subtracted optical density values for target proteins were normalized to β-actin to calculate relative expression levels. Each experiment was repeated three times independently.

2.5 α-KGDH activity

α-KGDH activities of jejunum samples were determined using colorimetric enzymatic activity assays (Sigma Aldrich, USA) according to the manufacturer's instructions.

2.6 Cell viability

Cell viability was determined by cell counting kit-8 (MCE, USA). Absorbance was measured at a wavelength of 450 nm by an enzyme linked immunosorbent assay reader (Bio-Rad, USA).

2.7 Measurement of Zn status

Intracellular Zn^{2+} level

Subsequent to Zn exposure, the cells were rinsed twice with PBS and incubated for 1 hour in PBS containing 1 μM fluozin^{TM}-3 AM (Life Technologies, USA), followed by a single PBS wash. The cell pellet was resuspended in 500 μl of PBS and intracellular Zn^{2+} level was analyzed by flow cytometer in the FITC channel (FACSCalibur, BD Biosciences).

Mitochondrial Zn^{2+} level

Following the overdose Zn treatment, the cells were washed twice with PBS and subsequently incubated for 20 min in PBS containing 1 μM fluozin^{TM}-3 AM. After the incubation, add 1 μL of MitoTracker (Life Technologies, USA) to the existing PBS staining solution and incubate for 40 minutes at 37°C. After the incubation period, images were captured using a fluorescence confocal microscope (Leica, Germany) in two channels: Ex/Em=644/665 nm and Ex/Em=494/516 nm.

2.8 Assessment of NAD^+ and ATP levels

Intracellular NAD^+ levels were assessed using the EnzyChrom NAD^+/NADH Assay Kit (BioAssay, USA), and ATP was detected using the CellTiter-Glo 2.0 Assay (Promega, USA), following the manufacturer's instructions.

2.9 Statistical analysis

The statistical analysis was performed utilizing SPSS 22.0 (IBM SPSS, Inc.). All data were presented as mean ± standard deviation (SD). Comparisons between two groups were performed using a *t* test. Comparisons between multiple groups were assessed through one-way ANOVA with post hoc Bonferroni testing unless otherwise indicated. A significance level of $P<0.05$ was considered indicative of a statistically significant difference.

3 Results

3.1 *In vivo*

3.1.1 Impact of imbalanced dietary Zn on Zn homeostasis-related protein expression in the intestine of mice

A dose-dependent elevation in serum zinc concentration was observed in mice with incremental dietary zinc supplementation (Figure S1). Zn homeostatic mechanisms primarily regulate excess Zn absorption through the internalization and degradation of the Zn uptake

protein ZIP4 [20; 21]. Additionally, metallothionein (MT), crucial for maintaining intracellular Zn stability, functions as both receptor and donor of Zn [22]. We initially examined the protein expression of ZIP4 and MT in the intestine of mice. Dietary Zn levels inversely correlate with ZIP4 expression and positively with MT expression, regardless of the duration of Zn intervention (Figure 1). Notably, high-Zn and excess-Zn diets significantly enhanced MT expression compared to the control-Zn group during short-term interventions (Figure 1D). Furthermore, during long-term interventions, low-Zn, high-Zn, and excess-Zn diets markedly affected the expression levels of ZIP4 and MT (Figure 1F-G), relative to the control group.

3.1.2 Impact of imbalanced dietary Zn on tight junction protein levels in the intestine of mice

Tight junction proteins such as ZO-1, Occludin, and Claudin-1 are pivotal in regulating paracellular permeability and maintaining barrier integrity [23]. To detect the effect of imbalance Zn on intestinal integrity in mice, we next measured the expression of ZO-1, Occludin, and Claudin-1. The expression levels of ZO-1 (Figure 1I) and Claudin-1 (Figure 1K) were significantly reduced in mice on low-Zn and excess-Zn diets compared to those on a control-Zn diet after four weeks. Besides, the high-Zn and excess-Zn groups showed a near-significant reduction in Occludin expression (Figure 1J). At eight weeks, the excess-Zn diet markedly decreased the expression of ZO-1 (Figure 1M) and Occludin (Figure 1N), while both high-Zn and excess-Zn diets significantly lowered Claudin-1 levels (Figure 1O).

3.1.3 Impact of imbalanced dietary Zn on oxidative stress in the intestine of mice

Oxidative stress was regarded as a primary factor in cell death induced by Zn deficiency. Therefore, we subsequently investigated the intestinal oxidative stress level of mice. In 4-week intervention, mice on a low-Zn diet exhibited significantly higher levels of ROS compared to those on a control-Zn diet, whereas high-Zn and excess-Zn diets did not increase ROS (Figure 2A-B). T-AOC was unchanged across all diets (Figure 2C). In addition, low-Zn diets significantly lowered MDA levels, with excess-Zn diets showing a similar trend (Figure 2D). NO levels were notably higher in mice on low-Zn and excess-Zn diets than those on control diets (Figure 2E). Over 8 weeks, ROS (Figure 2F-G) and NO (Figure 2J) remained elevated in low-Zn diets without significant changes in high-Zn or excess-Zn diets. T-AOC showed no variation across groups (Figure 2H), but high-Zn diets significantly raised MDA

levels compared to controls (Figure 2I).

To more precisely examine the intestinal oxidative stress level of mice, the expression levels of oxidative stress and antioxidant proteins were examined using Western blotting analysis. In short-term intervention, the excess-Zn diet significantly enhanced the protein expressions of NOX2 and phosphorylated Nrf2 (p-Nrf2), while decreasing Nrf2 expression compared to the control group (Figure 3A-D). In the 8-week samples, the effects on NOX2 and p-Nrf2 were not observed under excess-Zn conditions, although Nrf2 expression remained reduced. However, the impact of the low-Zn diet on these proteins aligned with the short-term effects observed in the excess-Zn group (Figure 3E-H).

3.1.4 Impact of imbalanced dietary Zn on the activity of α-KGDH in the intestine of mice

Since α-KGDH serves both as a source of mitochondrial ROS and a primary target for ROS in mitochondria, which is also a pivotal enzyme in the TCA cycle [24; 25], we investigated the change of α-KGDH activity in the intestine of mice. Our result showed that in short-term imbalanced Zn intervention, α-KGDH activity was significantly lower in both low-Zn and high-Zn diets compared to the control group, with a more pronounced decrease in the low-Zn group (Figure 3I). After 8 weeks, both low-Zn and excess-Zn diets markedly reduced α-KGDH activity compared to the control-Zn diet (Figure 3J).

3.2 *In vitro*

3.2.1 Dynamics of cytoplasmic oxidative stress in Zn overload treated IPEC-J2 cells

In order to clarify the predominant cause of Zn toxicity-induce cell death, we next detected the temporal dynamics of oxidative stress in Zn overload treated IPEC-J2 cells. Cellular ROS levels depicted a time dependent increase with the treatment of 150 μM $ZnSO_4$, reaching significant levels at 2 hours (Figure 4A-B). Figure 4C illustrated the alterations in the expression levels of cytoplasmic oxidative stress-related proteins at various treatment time points induced by Zn overload. The expression of protein kinase C (PKC) initiated an upward trajectory after 3 hours of exposure to 150 μM $ZnSO_4$, with a significant elevation observed by the 4-hour mark, surpassing the control group (Figure 4D). Additionally, the expression levels of the downstream protein NOXs can be seen in Figure 4E-F. The induction of Zn overload did not elicit a significant increase in NOX2 protein expression levels; rather,

there was an observable declining trend following 2 hours of Zn treatment (Figure 4E). The expression level of NOX4 protein was notably lower than that of the control group at the 2-hour time point. However, a reversal in this trend was evident at 3 hours, and after 4 hours of Zn treatment, its expression level markedly exceeded that of the control group (Figure 4F). Zn overload exhibited no appreciable impact on the protein expression levels of dual oxidase 2 (DUOX2) (Figure 4G).

We also detected the changes in the levels of cytoplasmic antioxidant-related proteins at different time points during Zn overload treatment. Our results showed that exposure to 150 μM $ZnSO_4$ resulted in a substantial upregulation of Nrf2 protein expression (Figure 4I). Subsequently, with the prolonged duration of Zn treatment, the expression level gradually diminished after 1 hour. Furthermore, Zn overload leads to a progressive reduction in p-Nrf2 expression, with the protein level being significantly lower than that in the control group after 4 hours of excessive Zn treatment (Figure 4J).

Although ROS can be generated by NOX in the cytoplasm, 90% of intracellular ROS originates from mitochondria [26]. In order to elucidate whether Zn can readily permeate mitochondria and subsequently trigger mitochondrial oxidative stress, we assessed mitochondrial Zn^{2+} levels in Zn overload treated IPEC-J2 cells. Mitochondrial Zn^{2+} significantly increased after excessive Zn treatment and gradually rise over time (Figure 5A-B). Next, we tested mitochondrial redox homeostasis. Mitochondrial ROS level exhibited a significant increase after two hours of Zn treatment (Figure 5C-D).

3.2.2 Dynamics of key enzymes in the TCA cycle, NAD^+ and ATP levels in Zn overload treated IPEC-J2 cells

The α-KGDH and its subunits are involved in the mitochondrial ROS production [27], and *in vivo* results showed that excess Zn inhibited the intestinal α-KGDH activities of mice. Consequently, we proceeded to examine the alterations in the expression levels of key components within the α-KGDH, namely OGDH, DLST and DLD, in Zn overload treated IPEC-J2 cells. OGDH expression levels exhibited a decline following 2 hours of excessive Zn treatment, with a significant reduction evident after 3 hours (Figure 6B). Zn overload had no significant impact on DLST protein expression levels (Figure 6C). Excessive Zn treatment induced a gradual decrease in DLD protein expression levels, and DLD expression was

notably lower than the control group after 2 hours of Zn intervention (Figure 6D). In addition, we also monitored the changes of IDH, another key enzyme of the TCA cycle. Similarly, after Zn treatment, there was a decrease in IDH1 expression levels, though no significant difference is observed (Figure 6E). IDH2 protein levels significantly decreased after 2 hours of excessive Zn treatment (Figure 6F).

NAD^+ is a key electron transporter which connects the TCA cycle to the electron transport chain [28; 29], and the TCA cycle processes are regulated by NAD^+ levels [30]. Hence, we hypothesized that the inhibition of α-KGDH and IDH expression levels might result from a reduction in NAD^+ levels. As expected, Zn overload lead to a significant reduction in NAD^+ levels, and this decrease exhibits a time-dependent manner (Figure 6G). Furthermore, after 2 hours of excessive Zn supplementation, a marked reduction in intracellular ATP concentration is observed (Figure 6H).

3.2.3 Supplementation of NAD^+ and its precursor, but not antioxidants, rescues Zn toxicity in IPEC-J2 cells

Furthermore, to examine whether oxidative stress or NAD^+ depletion was a primary contributor to Zn toxicity in IPEC-J2 cells, we evaluated the alleviating effects of antioxidants on Zn overload-induced cytotoxicity. Varying doses of dithiothreitol (DTT) did not alleviate Zn-induced cell death (Figure 7A). Moreover, vitamin E was also unable to rescue Zn-induced cytotoxicity (Figure 7B). In addition, we also used N-Acetylcysteine (NAC) to inhibit ROS and we found NAC indeed suppressed Zn-induced cell death (Figure 7C). However, the relieving effect of NAC was accomplished by chelating Zn^{2+} (Figure 7D-E). NAD^+ and its precursor nicotinamide mononucleotide (NMN) were also supplemented into IPEC-J2 cells with Zn overload exposure. As expected, both NMN and NAD^+ effectively mitigated the cellular damage caused by Zn overload (Figure 7F-G). Under conditions of 150 μM $ZnSO_4$ treatment for 4 hours, NAD^+ demonstrated a 100% efficiency in rescuing cells from Zn overload-induced cell death. To confirm that NMN and NAD^+ do not rescue cells from Zn overload-induced cell death by chelating Zn^{2+}, intracellular Zn^{2+} concentrations were measured. Neither NMN nor NAD^+ significantly affected intracellular Zn ion concentrations (Figure 7H-I). In addition, to our surprise, ferroptosis inhibitors, cuproptosis inhibitors, caspase-dependent inhibitors, necroptosis inhibitors, autophagy inhibitors, and disulfidptosis

inhibitors also failed to rescue cellular death induced by Zn overload (Figure S2). Consistent with these findings, no significant elevation of Caspase-3 was observed in murine models under high-zinc conditions, further corroborating that classical apoptotic pathways are not central to Zn toxicity (Figure S3F). It seems that the cytotoxicity induced by Zn overload may be associated with a death pathway separate from these well-established modes of cell death.

3.2.4 Dynamics of NAD^+ consumption and synthesis enzymes in Zn overload treated IPEC-J2 cells

The sirtuin protein family (SIRTs) are NAD^+-dependent histone deacetylases that play a pivotal role in numerous physiological processes, including apoptosis, mitochondrial biogenesis, and energy metabolism [31]. Figure 8A depicts the changes in SIRTs protein expression levels following Zn overload. SIRT1 protein levels began to decrease 2 hours after Zn treatment, and by 4 hours, its expression is significantly lower than in the control group (Figure 8B). Excessive Zn treatment notably impacted SIRT3 expression levels, with SIRT3 protein levels significantly lower than the control group after 1 hour of Zn intervention (Figure 8C). SIRT4 protein levels remained relatively unaffected by excessive Zn concentrations (Figure 8D). SIRT5 expression levels exhibited a significant reduction after 1 hour of Zn intervention, and this decrease persisted as the duration of Zn treatment prolongs (Figure 8E).

Over-production of ROS could induce the overactivation of PARP-1[32]. Excessive activation of PARP-1 necessitates a significant consumption of NAD^+ [33]. To investigate whether the Zn-induced cell death caused by NAD^+ depletion is associated with PARP-1 activation, we measured the changes of PARP-1-related protein expression levels in Zn overload treated IPEC-J2 cell (Figure 8F). PARP-1 expression levels significantly increased after 3 hours of excessive Zn treatment. Consistent with these findings, zinc overload also elicited a pronounced elevation in PARP-1 expression in murine models, underscoring the conserved role of PARP-1 activation across experimental systems (Figure S3A-C). However, downstream protein AIF expression levels did not exhibit a noticeable increase at 4 hours of Zn treatment (Figure 8H). These results indicate that the early reduction in NAD^+ levels is not directly linked to the activation of PARP-1. Furthermore, neither PARP-1 inhibitors nor AIF inhibitors can rescue cellular death induced by Zn overload (Figure 8I).

Cellular NAD^+ homeostasis is tightly regulated through a careful balance between its biosynthesis and degradation. In mammals, NAD^+ is synthesized through the de novo, Preiss-Handler, and salvage pathways [34]. The key enzymes in these biosynthetic pathways are nicotinamide phosphoribosyltransferase (NAMPT), nicotinamide mononucleotide adenylyltransferase (NMNAT) and quinolinate phosphoribosyltransferase (QPRT) [35]. To ascertain the reason for the decline in NAD^+ levels in Zn overload treated IPEC-J2 cell, we proceeded to measure the changes in the levels of key proteins involved in the synthesis of NAD^+, namely NMNAT1, QPRT and NAMPT (Figure 8J). Starting from 1 hour, excessive concentrations of Zn significantly reduced the expression level of NMNAT1 (Figure 8K). QPRT expression levels were similar to the control group from 1 to 3 hours of Zn intervention, but at 4 hours, it was significantly lower than that in the control group (Figure 8L). NAMPT expression gradually decreased with increasing Zn treatment duration, and after 2 hours, its expression level was significantly lower than that of the control group (Figure 8M).

3.2.5 Boosting NAD^+ synthesis rescue Zn toxicity in IPEC-J2 cells

To validate the depletion of NAD^+ level is a direct cause of Zn toxicity inIPEC-J2 cells and explore whether the reduction of key enzymes in NAD^+ synthesis pathway plays a pivotal role in it, NAMPT promoter NAT were used to promote the biosynthesis of NAD^+. As expected, NAT effectively alleviated cell death induced by Zn overload (Figure 9A). Indeed, NAT also considerably eased the Zn overload-induced diminishment of NAD^+ and ATP (Figure 9B-C). Additionally, Figure 9D depicts the protein expressions of key NAD^+ synthesis enzymes and SIRTs, we found NAT truly enhanced the protein expression of NAMPT (Figure 9E) and NAT remarkably reversed excess Zn-induced reductions in NAMPT, NMNAT1, QPRT, SIRT1, and SIRT5 protein expression levels but not significantly affected the protein level of SIRT3 (Figure 9 E-J). Moreover, to corroborate the above results, we also used overexpression plasmids to enhance the expression of NAMPT and NMNAT1. Although overexpressing via lipid carrier transfection didn't achieve very high transfection efficiency (Figure 9K-M), NMNAT1 and NAMPT overexpression still effectively mitigated the cytotoxicity induced by Zn overload to a certain extent (Figure 9N).

4 Discussion

Zn homeostatic mechanisms limit cellular Zn imbalance. The protein ZIP4 facilitates Zn uptake from both the extracellular environment and intracellular vesicles [36]. In response to elevated Zn levels, MT expression is activated, further regulating Zn balance by sequestering excess Zn [37]. Intestine ZIP4 expression decreased in a dose-dependent manner during both short-term and long-term interventions, whereas MT expression increased with higher dietary Zn concentrations, regardless of the duration of intervention. These alterations in Zn homeostatic mechanisms align with a moderate degree of imbalanced Zn intervention of mice.

Both inadequate and excessive amounts of Zn can disrupt Zn homeostasis, leading to diverse biological consequences. Our *in vivo* experiments have demonstrated that Zn imbalance resulted in a decline in intestinal tight junction proteins ZO-1, Occludin, and Claudin-1 of mice. Oxidative stress is recognized as the principal mechanism of cell death precipitated by Zn deficiency [38], whereas the pathways through which Zn excess contributes to cell death are still under debate. Whether under short-term or long-term Zn intervention, the Zn-deficient treated mice exhibited more severe oxidative damage to the intestine compared to the high Zn and Zn-excess groups, manifested by higher levels of ROS, MDA and NO in the Zn deficiency group. NOXs are regarded as the primary source of cellular ROS [39]. Given that in 4-week samples, the low-Zn group exhibited a relatively low protein expression level of NOX2, we hypothesized that this may be due to the presence of intracellular Zn stores [40], which maintain the activity of NOX2 during the early stages of Zn deficiency. Furthermore, the high expression of ZIP4 and low expression of MT in the low-Zn group also supported this hypothesis. In addition, consistent with the depletion of Zn reserves, sustained oxidative stress led to elevated NOX2 after 8 weeks. Conversely, the excess-Zn diet resulted in a high protein expression of NOX2, yet did not result in elevated ROS levels for 4 weeks. This phenomenon may be attributed to the activation of Nrf2 by NOX2, which has been identified as a crucial feedback loop to prevent ROS accumulation and oxidative-mediated cell damage [41]. After long-term consumption of excess-Zn diets, the disappearance of this phenomenon may be attributed to the fact that the body's Zn homeostasis enables the excretion of accumulated zinc, thus alleviating the excess Zn-induced damage. Additionally, we found that both short-term and long-term Zn imbalances

affect the activity of α-KGDH, a pivotal enzyme in the TCA cycle, with long-term Zn excess particularly causing severe damage to its activity. Collectively, the results suggested that both short-term and long-term Zn deficiency, as well as Zn excess, result in oxidative damage and impaired energy metabolism in the intestine of mice.

Given the well-documented mechanisms of cell death due to Zn deficiency, our subsequent research will focus on elucidating the mechanisms by which Zn overload induced cell death. To uncover the relationship between oxidative stress and energy metabolism impairment in the context of cell death induced by Zn overload, we detected the dynamics changes of oxidative stress and energy metabolism after Zn overload treatment in IPEC-J2 cells, which are ideal tools to study intestinal function and mimic the human physiology more closely than any other cell line of non-human origin. It has been reported that the abnormal accumulation of intracellular Zn^{2+} upregulates the expression of NOX1 protein, ultimately inducing senescence in vascular smooth muscle cells [8]. In neuronal cells, an excess of Zn can activate PKC, consequently leading to an elevation in NOX expression levels [7; 42]. However, in this experiment, the PKC-NOX oxidative stress pathway in IPEC-J2 cells was only activated during the later stages of Zn intervention. This indicates that, during the early stages of Zn overload, ROS may not be generated through the activation of cytoplasmic NOX.

Mitochondria serve as the cellular powerhouse, governing the TCA cycle, oxidative phosphorylation, and ATP synthesis [43]. They also occupy a central position in processes such as cellular apoptosis, differentiation, and innate immunity [44]. While our previous research confirmed that Zn overload can lead to a significant reduction in mitochondrial membrane potential [18], we still cannot ascertain whether Zn can directly enter mitochondria and affect mitochondrial function. In this experiment, a significant increase in mitochondrial Zn^{2+} levels was observed during the initial stages of Zn overload, indicating that Zn^{2+} can indeed target mitochondrial enzyme. We found a notable reduction in the protein expression levels of OGDH and DLD after 2 hours Zn overload treatment. Based on previous literature, deficiency in DLD leads to copious ROS production, resulting in metabolic imbalance and lactic acidosis [45; 46]. In this experiment, mitochondrial ROS levels significantly increased after 2 hours of Zn intervention, consistent with the activated state of DLD, which indicating that DLD may be a source of mitochondrial ROS production. IDH is also a key rate-limiting

enzyme in the TCA cycle, responsible for supplying essential energy and biosynthetic precursors for cellular metabolism. IDH1 is found in the cytoplasm and peroxisomes, crucial for sugar and lipid metabolism [47]. Meanwhile, IDH2 primarily resides in the mitochondrial matrix, playing a vital role in maintaining redox balance by generating NADPH [48]. We found that Zn overload had a negative impact on IDH2, while IDH1 was not significantly affected by excessive Zn concentrations, highlighting that excess Zn can selectively target mitochondria in IPEC-J2 cells.

The TCA cycle is strictly regulated by the levels of NAD^+, which, in turn, impacts α-KGDH and IDH within the mitochondria [30; 49]. NAD^+, a central coenzyme in cellular redox reactions and energy metabolism, plays a pivotal role in maintaining mitochondrial function and genomic stability[50]. In the present study, NAD^+ levels significantly decreased after 1 hour of Zn intervention, showing a time-dependent manner. Recent studies have established that NAD^+ depletion is a hallmark of multiple regulated cell death pathways. Zhao et al. revealed that ferroptosis, traditionally viewed as iron-dependent lipid peroxidation, can also be driven by NAD^+ deficiency in metabolically stressed cancer cells[51]. Emerging studies have identified NAD^+ depletion as a central mechanism driving cell death in Niemann-Pick type C1 (NPC1) disease[52]. In order to investigate whether the reduction in NAD^+ levels is the primary cause of cell death induced by Zn overload, we assessed the rescuing effect of NAD^+ supplements on Zn overload-induced cell death. Interestingly, both NAD^+ and its precursor (NMN) effectively rescued Zn-induced IPEC-J2 cell death, with NAD^+ achieving a rescue rate close to 100%. Moreover, the addition of NMN and NAD^+ did not impact intracellular Zn^{2+} concentrations, indicating that NAD^+ and NMN do not rescue Zn-induced cytotoxicity through chelation of intracellular Zn^{2+}. Another interesting finding is that the application of antioxidants (Vitamin E and DTT) did not ameliorate Zn-induced cell death, implying that oxidative stress may not be the primary underlying cause of cell death induced by excess Zn. Although ROS inhibitor NAC truly alleviated Zn overload induced cell death, this effect depended to a great extent on decreasing the levels of Zn^{2+} by chelating Zn^{2+}. Thus, we suggest that the primary underlying factor leading to cell death in IPEC-J2 cells induced by Zn overload is the reduction in NAD^+ levels, which didn't mean the denial of the role of ROS production in it.

SIRTs are NAD^+-dependent deacylases with a wide range of functions in transcription regulation, energy metabolism modulation, cell survival, and DNA repair [53]. SIRT1 is found in the nucleus and serves as a crucial regulator of lipid and glucose metabolism, while SIRT3, 4, and 5 are located in the mitochondria and have roles in oxidative stress and cell death [54; 55]. As expected, excessive Zn suppressed the expression of SIRT1, SIRT3, and SIRT5, with a notable drop in SIRT3 and SIRT5 levels observed after just 1 hour of Zn exposure, implicating that energy metabolism impairment occurs in the early stages of Zn overload. PARP-1 functions at the center of cellular stress responses, where it processes a multitude of signals and, in response, directs cells to specific fates (e.g., DNA repair vs. cell death) [56]. Moreover, the activation of PARP-1 involves substantial NAD^+ consumption [57]. A previous study showed that excess Zn could stimulate PARP-1 in microglial cells [58]. Consequently, we hypothesize that Zn overload induces cell death via PARP-1 activation, NAD^+ depletion and AIF release. However, PARP-1 stimulation occurred in the late stages of Zn overload, and unfortunately, inhibitors of AIF and PARP-1 cannot fully rescue Zn-induced cytotoxicity. Thus, we believed that although PARP-1 is involved in the process of Zn-induced cell death, it is not the main cause of Zn-induced cytotoxicity.

In order to explore the primary factor behind Zn overload-induced NAD^+ depletion and subsequent cell death, we examined key proteins in the NAD^+ synthesis pathway. The salvage pathway represents the predominant source of NAD^+ due to its high adaptability. In this pathway, nicotinamide is enzymatically converted into NMN by intracellular NAMPT [59]. Subsequently, NMN, together with ATP, is transformed into NAD^+ by the second enzyme, NMNAT [60]. In the present study, NAD^+ salvage pathway was inhibited in the early stages of Zn overload. NAMPT is critically required for the maintenance of cellular NAD^+ supply catalysing the rate-limiting step of the NAD^+ salvage pathway. As expected, NAMPT activator NAT exhibited a robust rescue effect in Zn overload condition. Moreover, NAMPT and NMNAT1 overexpression also slightly rescued Zn overload-induced cytotoxicity, despite the relatively low efficiency of overexpression. It has been reported that overexpressing NMNAT1 lowers the sensitivity of neurons to the cytotoxicity of 40 μM Zn, but it fails to rescue neuronal cells under the treatment condition of 400 μM [61]. QPRT is a key enzyme in NAD^+ de novo synthesis pathway, in the present study, QPRT were suppressed in the late

stage of Zn overload [62]. Therefore, we deduce that excessive Zn inhibits the NAD^+ synthesis pathway, particularly the NAD^+ salvage pathway, leading to a decrease in NAD^+ levels and subsequently inducing cell death. These observations position zinc overload as a systemic disruptor of metabolic networks. Beyond the intestine, zinc dyshomeostasis may similarly impair NAD^+-dependent processes in other tissues, such as hepatic lipid oxidation regulated by SIRT1 or neuronal redox balance governed by SIRT3, as evidenced in models of metabolic and neurodegenerative diseases[63; 64]. Furthermore, zinc's ability to bind and inhibit metabolic enzymes—such as α-KGDH in the TCA cycle—highlights its broader role as a modulator of cellular metabolism, potentially altering substrate utilization in glucose, lipid, and amino acid pathways[65]. To unravel zinc's multifaceted metabolic effects, future studies should prioritize multi-omics approaches to map tissue-specific vulnerabilities. Comparative analyses of intestinal epithelia, hepatocytes, and neurons could clarify why certain cells are more susceptible to NAD^+ depletion.

In the past decade, the correlation between trace elements and cell death has emerged as a focal point in the field of life sciences. Dixon et al. [66] reported a form of iron-dependent cell death known as ferroptosis, characterized by iron accumulation and lipid peroxidation driving a programmed cell death process[67]. Tsvetkov et al. [68] unveiled cuprotosis, where copper ions binding to acylated components in the TCA cycle cause abnormal protein aggregation and loss of iron-sulfur cluster proteins, initiating toxic stress responses and cell death. A very recent study introduced disulfidptosis, excessive disulfide bond accumulation disrupts actin-cytoskeletal cross-linking, causing cytoskeletal contraction, structural disruption, and eventual cell death [69]. Interestingly, inhibitors of ferroptosis, cuproptosis, disulfidptosis (DTT), as well as apoptosis, autophagy, pyroptosis and necroptosis, all failed to rescue Zn overload-induced cell death. These results indicate that Zn appears to have a novel non-canonical death pathway. Further investigation is warranted to elucidate the association between Zn and cell death manner.

5 Conclusion

In general, our findings indicate that excessive Zn increases the levels of Zn^{2+} in mitochondria, then impedes NAD^+ synthesis enzyme NAMPT, leading to a reduction in NAD^+ levels and its dependent deacylases, SIRT3 and SIRT5, which in turn affects the TCA

cycle in mitochondria and disrupts cellular redox balance. Furthermore, in the nucleus, the overproduction of ROS activates PARP-1. Excessive Zn also interferes with the synthesis of NAD^+ enzymes, NAMPT and NMNAT1, which results in a reduction of NAD^+ levels and its dependent deacylases SIRT1. The reduction of NAD^+ levels ultimately triggers cell death and intestinal damage. NAD^+ supplement may serve as an effective intervention to rescue and alleviate Zn toxicity.

Acknowledgements

We would like to thank the National Key Technologies R & D Program of China (2022YFD1300500), and the National Natural Science Foundation of China (No. 31972998) for financial support. We also thank Figdraw as the graphical abstract was drawn by Figdraw.

Author Contributions

Jie Feng directed the project and acquired the funding. Jie Feng, Lingjun Chen and Feifei Huang designed the experiments. Lingjun Chen, Feifei Huang, Leilei Zhu, Xin Tian and Mohan Zhou conducted experiments. All authors discussed the results. Feifei Huang and Lingjun Chen performed the analysis of the data, generated the figures and wrote the original manuscript. All authors reviewed and approved the final paper.

Competing Interests

The authors declare that there is no conflict of interest.

References

Choi S., Liu X., & Pan Z. (2018) Zinc deficiency and cellular oxidative stress: prognostic implications in cardiovascular diseases. Acta Pharmacologica Sinica, 39(7), 1120-1132.

Zhang Y., Song M., Mucci L., A et al (2022) Zinc supplement use and risk of aggressive prostate cancer: a 30-year follow-up study. European Journal of Epidemiology, 37(12), 1251-1260.

Bailey R.L., Catellier D.J., Jun S.Y. et al (2018) Total Usual Nutrient Intakes of US Children (Under 48 Months): Findings from the Feeding Infants and Toddlers Study (FITS) 2016. Journal of Nutrition, 148, 1557-1566.

Kloubert V., Blaabjerg K., Dalgaard T.S. et al (2018) Influence of zinc supplementation on immune parameters in weaned pigs. Journal of Trace Elements in Medicine and Biology, 49, 231-240.

Huang X., Jiang D., Zhu Y. et al (2017) Chronic high dose zinc supplementation induces visceral adipose tissue hypertrophy without altering body weight in mice. Nutrients, 9(10), 1138.

Narayanan S.E., Rehuman N.A., Harilal S. et al (2020) Molecular mechanism of zinc neurotoxicity in Alzheimer's disease. Environmental Science and Pollution Research, 27(35), 43542-43552.

Noh K.M., & Koh J.Y. (2000) Induction and activation by zinc of NADPH oxidase in cultured cortical neurons and astrocytes. Journal of Neuroscience, 20(23), 1-5.

Salazar G., Huang J., Feresin R.G. et al (2017) Zinc regulates Nox1 expression through a NF-κB and mitochondrial ROS dependent mechanism to induce senescence of vascular smooth muscle cells. Free Radical Biology and Medicine, 108, 225-235.

Kondo K., Obitsu S., Ohta S. et al (2010) Poly(ADP-ribose) Polymerase (PARP)-1-independent Apoptosis-inducing Factor (AIF) Release and Cell Death Are Induced by Eleostearic Acid and Blocked by α-Tocopherol and MEK Inhibition. Journal of Biological Chemistry, 285(17), 13079-13091.

Rudolf E., Rudolf K., & Cervinka M. (2005) Zinc induced apoptosis in HEP-2 cancer cells: The role of oxidative stress and mitochondria. BioFactors, 23(2), 107-120.

Kim Y.H., & Koh J.Y. (2002) The role of NADPH oxidase and neuronal nitric oxide synthase in zinc-induced poly(ADP-ribose) polymerase activation and cell death in cortical culture. Experimental Neurology, 177(2), 407-418.

Yu S.W., Andrabi S.A., Wang H. et al (2006) Apoptosis-inducing factor mediates poly(ADP-ribose) (PAR) polymer-induced cell death. Proceedings of the National Academy of Sciences of the United States of America, 103(48), 18314-18319.

Koh J.Y. (2001) Zinc and disease of the brain. Molecular Neurobiology, 24(1-3), 99-106.

Lemire J., Mailloux R., & Appanna V.D. (2008) Zinc-toxicity alters mitochondrial metabolism and leads to decreased ATP production in hepatocytes. Journal of Applied Toxicology, 28(2), 175-182.

Dineley K.E., Votyakova T.V., & Reynolds I.J. (2003) Zinc inhibition of cellular energy production: implications for mitochondria and neurodegeneration. Journal of Neurochemistry, 85(3), 563-570.

Zhou X., Li Y.S., Li Z.J. et al (2017) Effect of dietary zinc on morphological characteristics and apoptosis related gene expression in the small intestine of Bama miniature pigs. Acta Histochemica, 119(3), 235-243.

Yang P.F., Hong W.D., Zhou P. et al (2017) Nano and bulk ZnO trigger diverse Zn-transport-related gene transcription in distinct regions of the small intestine in mice after oral exposure. Biochemical and Biophysical Research Communications, 493(3), 1364-1369.

Chen L.J., Yu X.N., Ding H.X. et al (2020) Comparing the influence of high doses of different zinc salts on oxidative stress and energy depletion in IPEC-J2 cells. Biological Trace Element Research, 196(2), 481-493.

Chen L.J., Wang Z.H., Wang P. et al (2021) Effect of Long-Term and Short-Term Imbalanced Zn Manipulation on Gut Microbiota and Screening for Microbial Markers Sensitive to Zinc Status. Microbiology Spectrum, 9(3).

Kambe T., Tsuji T., Hashimoto A. et al (2015) The physiological, biochemical, and molecular roles of zinc transporters in zinc homeostasis and metabolism. Physiological Reviews, 95(3), 749-784.

Huang T.L., Yan G.Y., & Guan M. (2020) Zinc homeostasis in bone: zinc transporters and bone diseases. International Journal of Molecular Sciences, 21(4), 1236-1247.

Pei X.Y., Jiang H.Y., Li C. et al (2023) Oxidative stress-related canonical pyroptosis pathway, as a target of liver toxicity triggered by zinc oxide nanoparticles. Journal of Hazardous Materials, 442, 18.

Chelakkot C., Ghim J., & Ryu S.H. (2018) Mechanisms regulating intestinal barrier integrity and its pathological implications. Experimental & molecular medicine, 50(8), 1-9.

Horvath G., Svab G., Komlódi T. et al (2022) Reverse and forward electron flow-induced H_2O_2 formation is decreased in α-ketoglutarate dehydrogenase (α-KGDH) subunit (E2 or E3) heterozygote knock out animals. Antioxidants, 11(8), 1487-1505.

Tretter L., & Adam-Vizi V. (2005) Alpha-ketoglutarate dehydrogenase: a target and generator of oxidative stress. Philosophical Transactions of the Royal Society B-Biological Sciences, 360(1464), 2335-2345.

Zhang W.J., Hu X.L., Shen Q. et al (2019) Mitochondria-specific drug release and reactive oxygen species burst induced by polyprodrug nanoreactors can enhance chemotherapy. Nature Communications, 10(1), 14.

Horvath G., Svab G., Komlódi T. et al (2022) Reverse and Forward Electron Flow-Induced H₂O₂ Formation Is Decreased in α-Ketoglutarate Dehydrogenase (α-KGDH) Subunit (E2 or E3) Heterozygote Knock Out Animals. Antioxidants, 11(8), 19.

Kory N., de Bos J.U., van der Rijt S. et al (2020) MCART1/SLC25A51 is required for mitochondrial NAD transport. Science Advances, 6(43), 14.

Klabunde B., Wesener A., Bertrams W. et al (2023) NAD^+ metabolism is a key modulator of bacterial respiratory epithelial infections. Nature Communications, 14(1), 5818.

Navas L.E., & Carnero A. (2021) NAD^+ metabolism, stemness, the immune response, and cancer. Signal Transduction and Targeted Therapy, 6(1), 2.

Morigi M., Perico L., & Benigni A. (2018) Sirtuins in renal health and disease. Journal of the American Society of Nephrology, 29(7), 1799-1809.

Li D., Kou Y., Gao Y. et al (2021) Oxaliplatin induces the PARP1-mediated parthanatos in oral squamous cell carcinoma by increasing production of ROS. Aging (Albany NY), 13(3), 4242-4257.

Joseph A., Juncheng P., Mondini M. et al (2021) Metabolic features of cancer cells impact immunosurveillance. Journal for immunotherapy of cancer, 9(6).

Zapata-Pérez R., Wanders R.J.A., van Karnebeek C.D.M. et al (2021) NAD^+ homeostasis in human health and disease. Embo Molecular Medicine, 13(7), 15.

Cambronne X.A., & Kraus W.L. (2020) Location, location, location: compartmentalization of NAD^+ synthesis and functions in mammalian cells. Trends in Biochemical Sciences, 45(10), 858-873.

Zhang T., Sui D., & Hu J. (2016) Structural insights of ZIP4 extracellular domain critical for optimal zinc transport. Nature Communications, 7, 11979.

Maret W., & Krezel A. (2007) Cellular zinc and redox buffering capacity of metallothionein/thionein in health and disease. Molecular medicine (Cambridge, Mass.), 13(7-8), 371-375.

Wedler N., Matthäus T., Strauch B. et al (2021) Impact of the cellular zinc status on PARP-1 activity and genomic stability in HeLa S3 cells. Chemical Research in Toxicology, 34(3), 839-848.

Selemidis S., Sobey C.G., Wingler K. et al (2008) NADPH oxidases in the vasculature: molecular features, roles in disease and pharmacological inhibition. Pharmacology & Therapeutics, 120(3), 254-291.

Slepchenko K.G., Lu Q., & Li Y.V. (2017) Cross talk between increased intracellular zinc (Zn(2+)) and accumulation of reactive oxygen species in chemical ischemia. American Journal of Physiology: Cell Physiology, 313(4), 448-459.

Smyrnias I., Zhang X., Zhang M. et al (2015) Nicotinamide adenine dinucleotide phosphate oxidase-4-dependent upregulation of nuclear factor erythroid-derived 2-like 2 protects the heart during chronic pressure overload. Hypertension, 65(3), 547-553.

Noh K.M., Kim Y.H., & Koh J.Y. (1999) Mediation by membrane protein kinase C of zinc-induced oxidative neuronal injury in mouse cortical cultures. Journal of Neurochemistry, 72(4), 1609-1616.

Rath E., Moschetta A., & Haller D. (2018) Mitochondrial function - gatekeeper of intestinal epithelial cell homeostasis. Nature Reviews Gastroenterology & Hepatology, 15(8), 497-516.

Spinelli J.B., & Haigis M.C. (2018) The multifaceted contributions of mitochondria to cellular metabolism. Nature Cell Biology, 20(7), 745-754.

Ambrus A., & Adam-Vizi V. (2018) Human dihydrolipoamide dehydrogenase (E3) deficiency: Novel insights into the structural basis and molecular pathomechanism. Neurochemistry International, 117, 5-14.

Szabo E., Wilk P., Nagy B. et al (2019) Underlying molecular alterations in human dihydrolipoamide dehydrogenase deficiency revealed by structural analyses of disease-causing enzyme variants. Human Molecular Genetics, 28(20), 3339-3354.

Medeiros B.C., Fathi A.T., DiNardo C.D. et al (2017) Isocitrate dehydrogenase mutations in myeloid malignancies. Leukemia, 31(2), 272-281.

Cairns R.A., & Mak T.W. (2013) Oncogenic Isocitrate Dehydrogenase Mutations: Mechanisms, Models, and Clinical Opportunities. Cancer Discovery, 3(7), 730-741.

Chen H.L., Denton T.T., Xu H. et al (2016) Reductions in the mitochondrial enzyme -ketoglutarate dehydrogenase complex in neurodegenerative disease - beneficial or detrimental? Journal of Neurochemistry, 139(5), 823-838.

Sundaram B., Pandian N., Kim H.J. et al (2024) NLRC5 senses NAD plus plus depletion, forming a PANoptosome and driving PANoptosis and inflammation. Cell, 187(15).

Yu J., Zhong B.L., Zhao L. et al (2023) Fighting drug-resistant lung cancer by induction of NAD(P)H:quinone oxidoreductase 1 (NQO1)-mediated ferroptosis. Drug Resistance Updates, 70.

Kataura T., Sedlackova L., Sun C.X. et al (2024) Targeting the autophagy-NAD axis protects against cell death in Niemann-Pick type C1 disease models. Cell Death & Disease, 15(5).

Noh M., Sim J.Y., Kim J. et al (2024) Particulate matter-induced metabolic recoding of epigenetics in macrophages drives pathogenesis of chronic obstructive pulmonary disease. Journal of Hazardous Materials, 464, 23.

Kitade M., Ogura Y., Monno I. et al (2019) Sirtuins and Type 2 Diabetes: Role in Inflammation, Oxidative Stress, and Mitochondrial Function. Frontiers in Endocrinology, 10, 12.

Parihar P., Solanki I., Mansuri M.L. et al (2015) Mitochondrial sirtuins: emerging roles in metabolic regulations, energy homeostasis and diseases. Experimental Gerontology, 61, 130-141.

Sun H.X., Liu C., Han F. et al (2023) The regulation loop of MARVELD1 interacting with PARP1 in DNA damage response maintains genome stability and promotes therapy resistance of cancer cells. Cell Death and Differentiation, 30(4), 922-937.

Kim M.Y., Mauro S., Gévry N. et al (2004) NAD^+-dependent modulation of chromatin structure and transcription by nucleosome binding properties of PARP-1. Cell, 119(6), 803-814.

Mortadza S.S., Sim J.A., Stacey M. et al (2017) Signalling mechanisms mediating Zn^{2+}-induced TRPM2 channel activation and cell death in microglial cells. Scientific Reports, 7, 15.

Verdin E. (2015) NAD^{+} in aging, metabolism, and neurodegeneration. Science, 350(6265), 1208-1213.

Gerner R.R., Klepsch V., Macheiner S. et al (2018) NAD metabolism fuels human and mouse intestinal inflammation. Gut, 67(10), 1813-1823.

Cai A.L., Zipfel G.J., & Sheline C.T. (2006) Zinc neurotoxicity is dependent on intracellular NAD^{+} levels and the sirtuin pathway. European Journal of Neuroscience, 24(8), 2169-2176.

Mehr A.P., Tran M.T., Ralto K.M. et al (2018) De novo NAD^{+} biosynthetic impairment in acute kidney injury in humans. Nature Medicine, 24(9), 1351-1359.

Rosenkranz E., Metz C.H.D., Maywald M. et al (2016) Zinc supplementation induces regulatory T cells by inhibition of Sirt-1 deacetylase in mixed lymphocyte cultures. Molecular Nutrition & Food Research, 60(3), 661-671.

Stegger L., Eilers F., Schaeg F. et al (2024) Radiation protection during liver surgery shortly after SIRT: Interactive visualization of radiation on the liver surface for individualized planning. European Journal of Nuclear Medicine and Molecular Imaging, 51, S426-S427.

Gazaryan I.G., Krasinskaya I.P., Kristal B.S. et al (2007) Zinc irreversibly damages major enzymes of energy production and antioxidant Defense prior to mitochondrial permeability transition. Journal of Biological Chemistry, 282(33), 24373-24380.

Dixon S.J., Lemberg K.M., Lamprecht M.R. et al (2012) Ferroptosis: An Iron-Dependent Form of Nonapoptotic Cell Death. Cell, 149(5), 1060-1072.

Liu S., Lai X., Xue X. et al (2025) Embryonic development mediated by ferroptotic trigger waves. The Innovation Life, 3(1), 100114.

Tsvetkov P., Coy S., Petrova B. et al (2022) Copper induces cell death by targeting lipoylated TCA cycle proteins. Science, 375(6586), 1254-1261.

Liu X.G., Nie L.T., Zhang Y.L. et al (2023) Actin cytoskeleton vulnerability to disulfide stress mediates disulfidptosis. Nature Cell Biology, 25(3), 404-414.

Figures

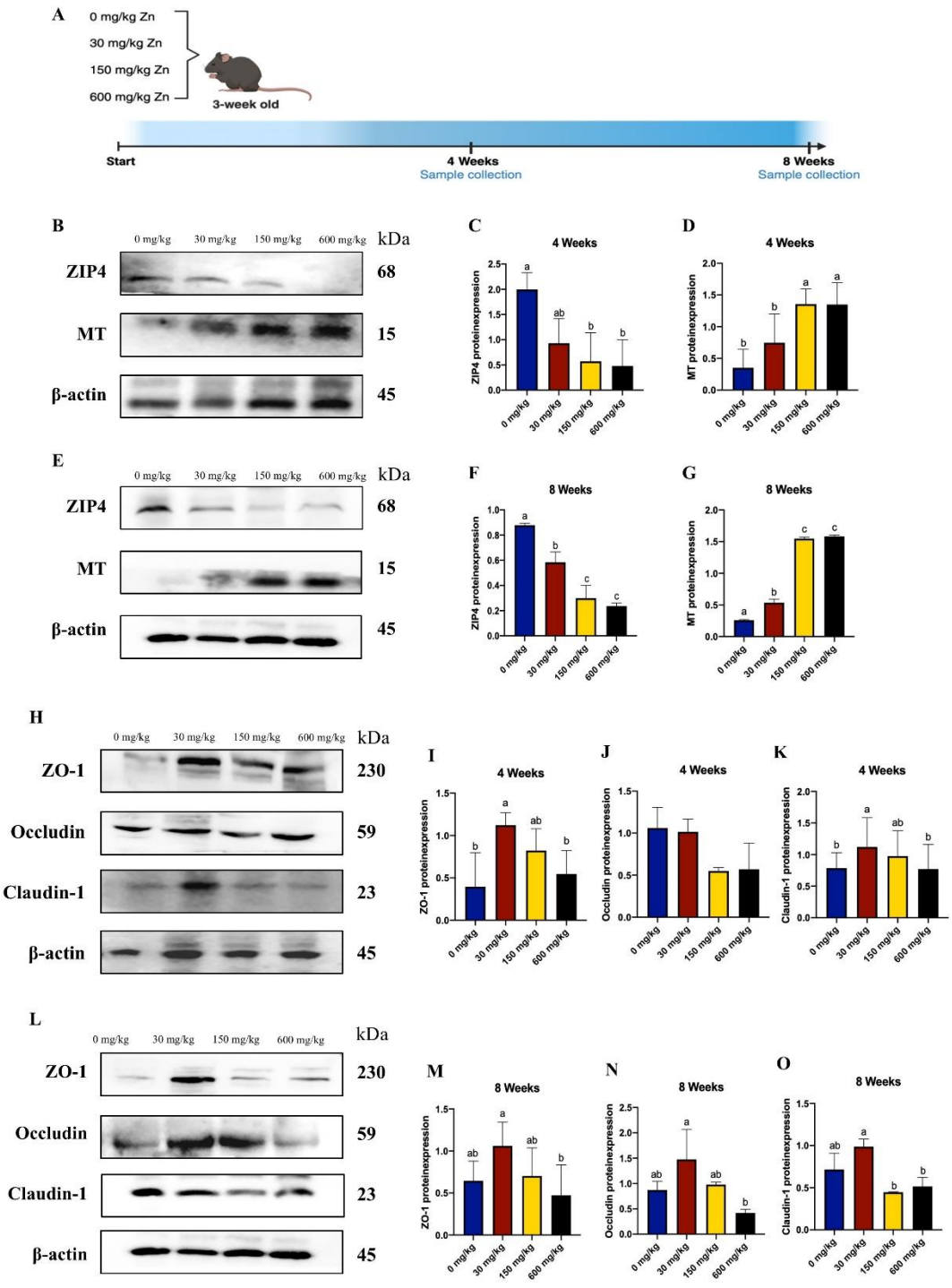

Fig. 1 Effect of imbalanced dietary Zn on Zn transporter and tight junction protein. Experimental design of short-term and long-term Zn imbalance in mice (A). The expression levels of ZIP4 and MT in short-term Zn intervention (B-D). The expression levels of ZIP4 and MT in long-term Zn intervention (E-G). Results are given as mean ± SD (n=3-4). The expression levels of ZO-1, Occludin, and Claudin-1 in short-term Zn intervention (H-K). The expression levels of ZO-1, Occludin, and Claudin-1 in long-term Zn

intervention (L-O). Results are given as mean ± SD (n=3-5). Groups labeled without a common letter were significantly different (P<0.05).

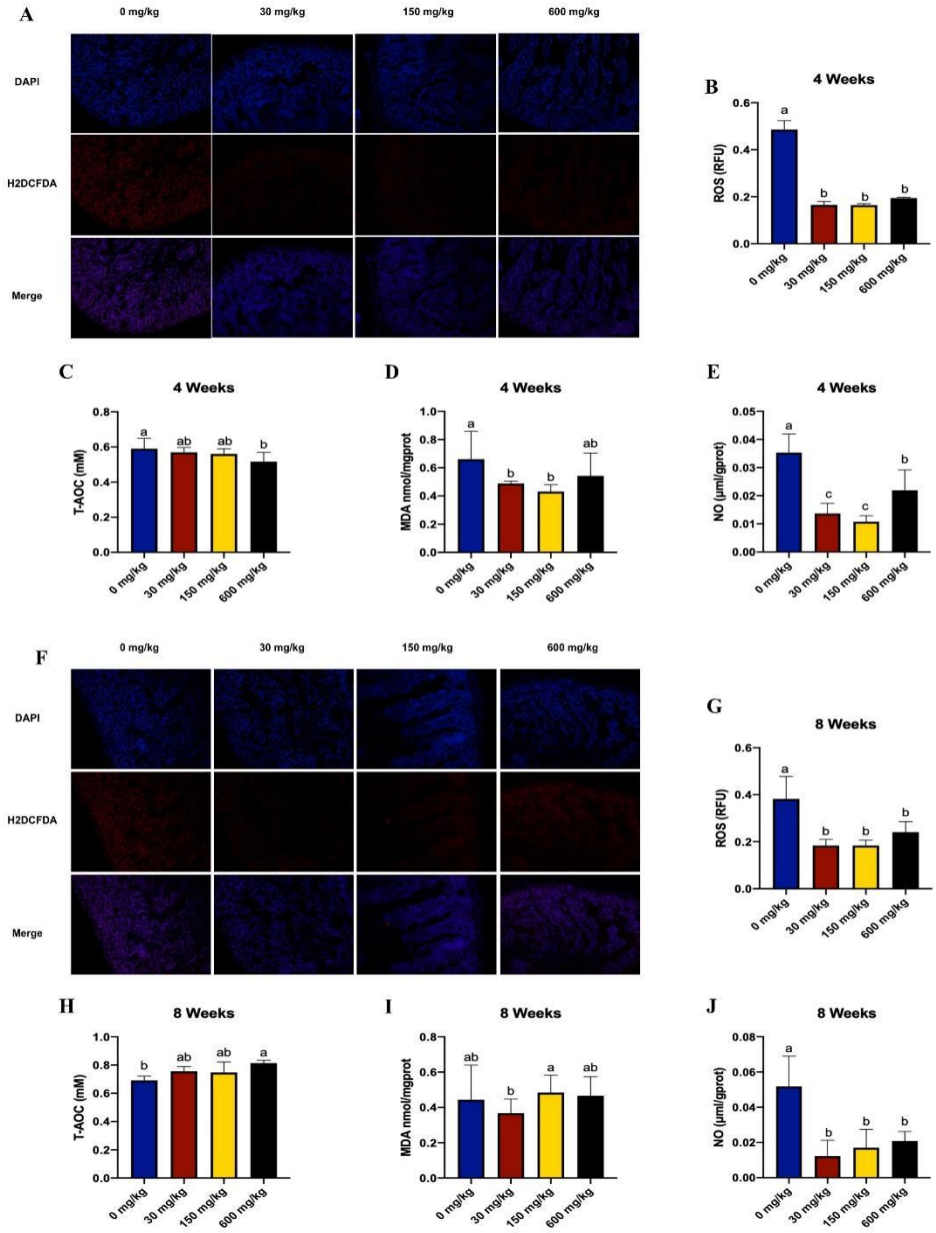

Fig. 2 Effect of imbalanced dietary Zn on oxidative stress indicators. The levels of ROS (A-B), T-AOC (C), MDA (D) and NO (E) in short-term Zn intervention. The expression levels of ROS (F-G), T-AOC (H), MDA (I) and NO (J) in long-term Zn intervention. Results are given as mean ± SD (n=4-8). Groups labeled without a common letter were significantly different (P<0.05).

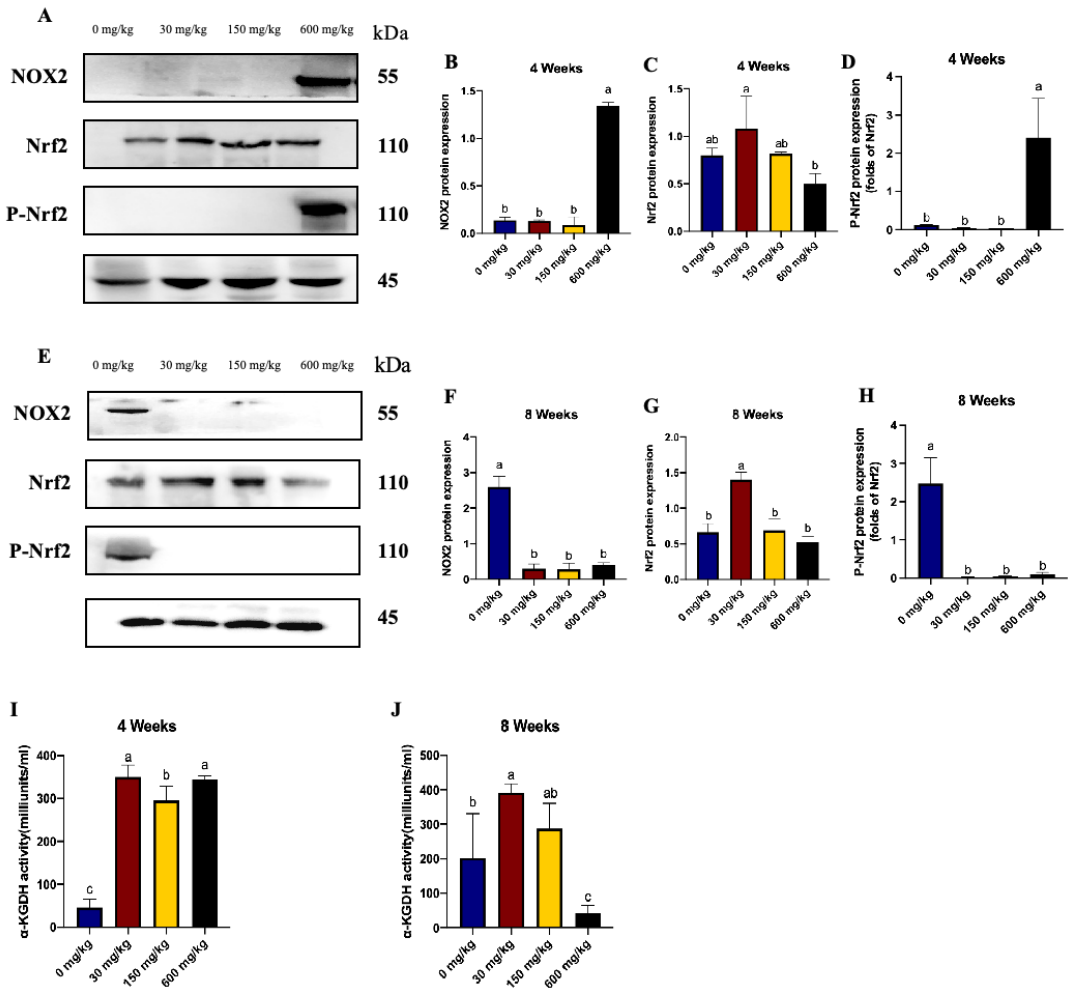

Fig. 3 Effect of imbalanced dietary Zn on oxidative stress related protein and α-KGDH. The expression levels of NOX2, Nrf2, and P-Nrf2 in short-term Zn intervention (A-D). The expression levels of NOX2, Nrf2, and P-Nrf2 in long-term Zn intervention (E-H). The activities of α-KGDH in short-term Zn intervention (I). The activities of α-KGDH in long-term Zn intervention (J). Results are given as mean ± SD (n=3). Groups labeled without a common letter were significantly different (P<0.05).

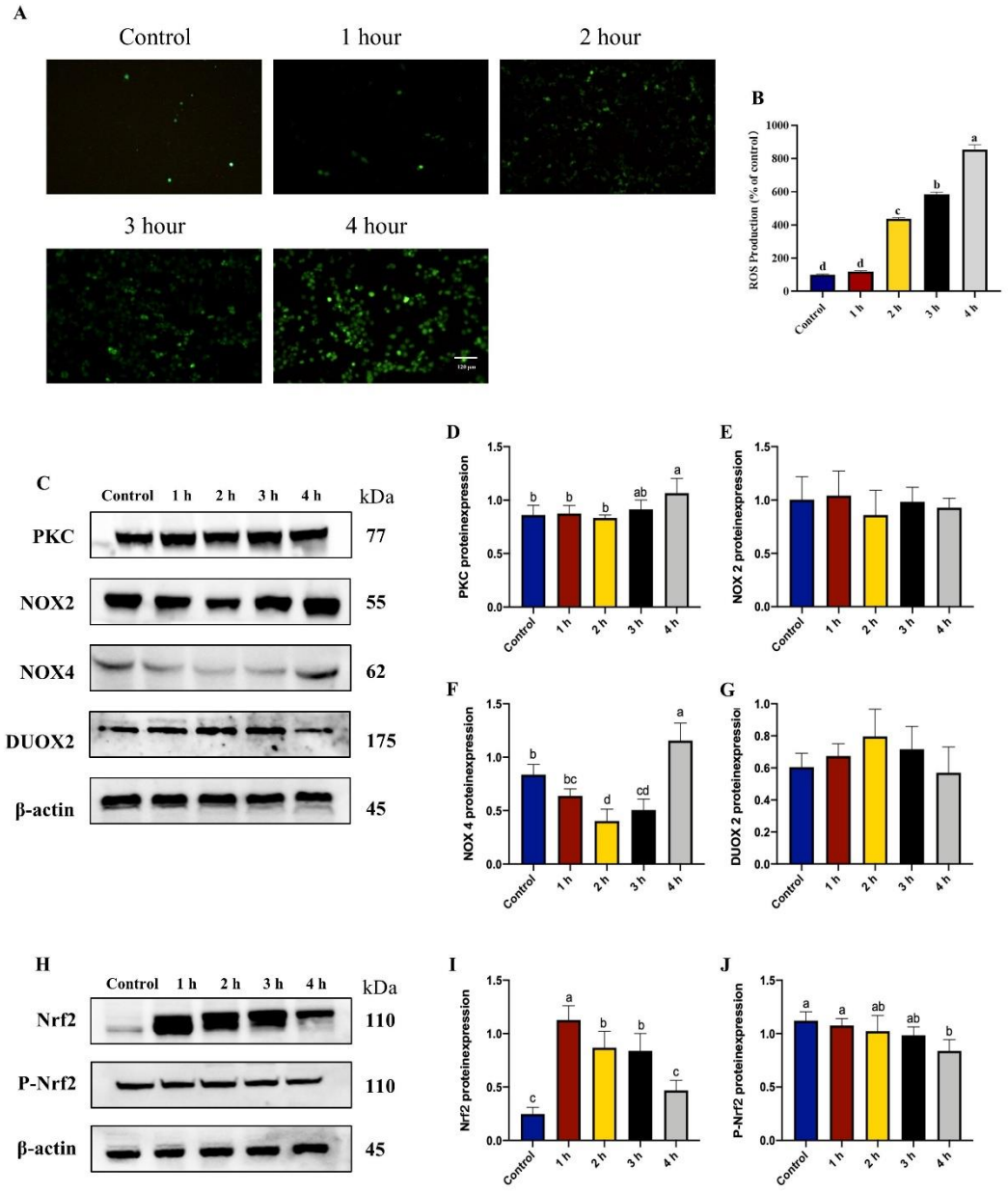

Fig. 4 Changes in cellular ROS levels and the expression levels of oxidative stress-related proteins following Zn treatment. Change of cellular ROS levels at various time intervals following Zn overload (A). Quantification of cellular ROS (B). Alterations in protein expression levels of cytoplasmic oxidative stress-related proteins at various time intervals following Zn overload, including PKC, NOX2, NOX2, and DUOX2 (C-G). Alterations in protein expression levels of cytoplasmic antioxidant-related proteins at various time intervals following Zn overload, including Nrf2, and P-Nrf2 (H-J). Results are given as mean ± SD (n=3-5). Groups labeled without a common letter were significantly different (P<0.05).

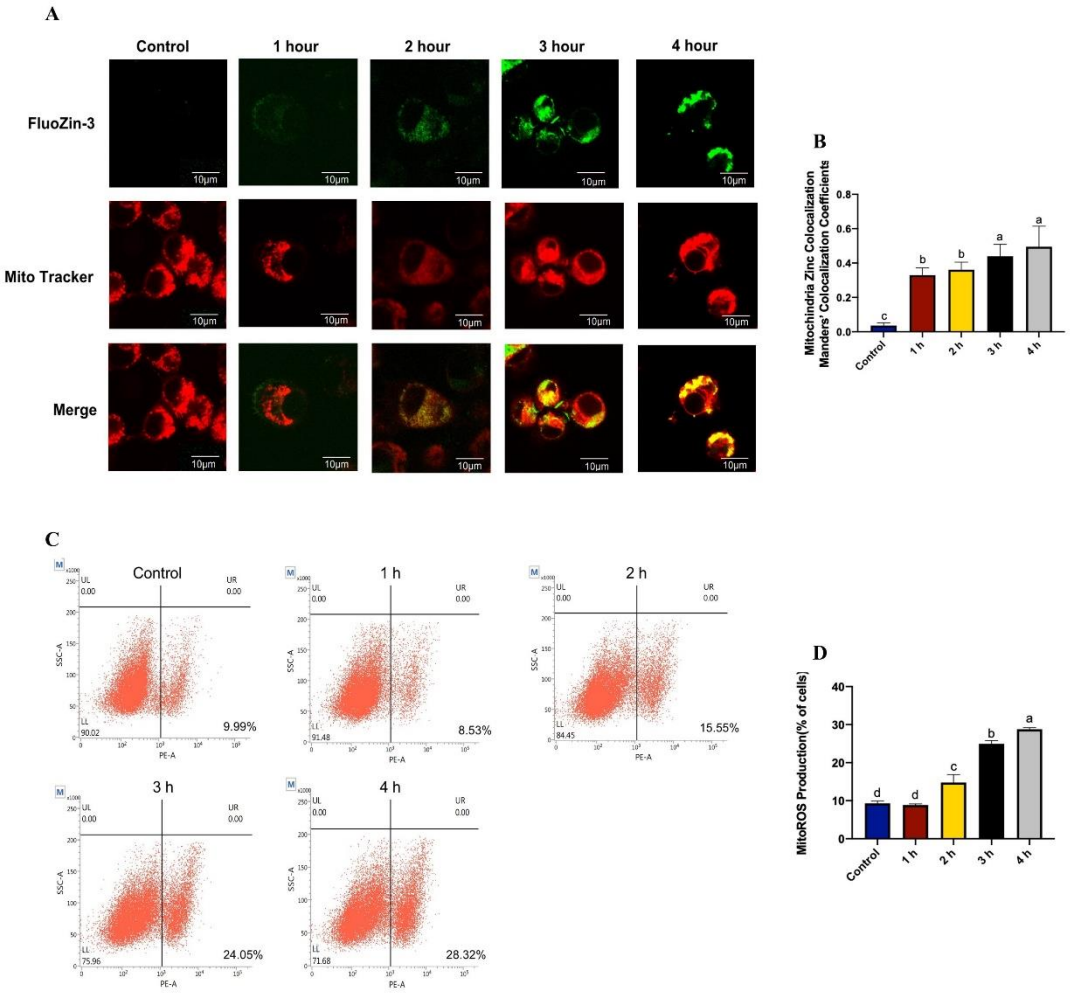

Fig. 5 Changes in status of mitochondrial Zn^{2+} and ROS following Zn treatment. Mitochondrial Zn^{2+} levels were determined through co-localization using MitoTracker and Fluozin-3 fluorescence (A). Quantification of mitochondrial Zn^{2+} (B). Flow cytometric analysis of mitochondrial ROS (C). Quantification of mitochondrial ROS (D); groups labeled without a common letter were significantly different (P<0.05).

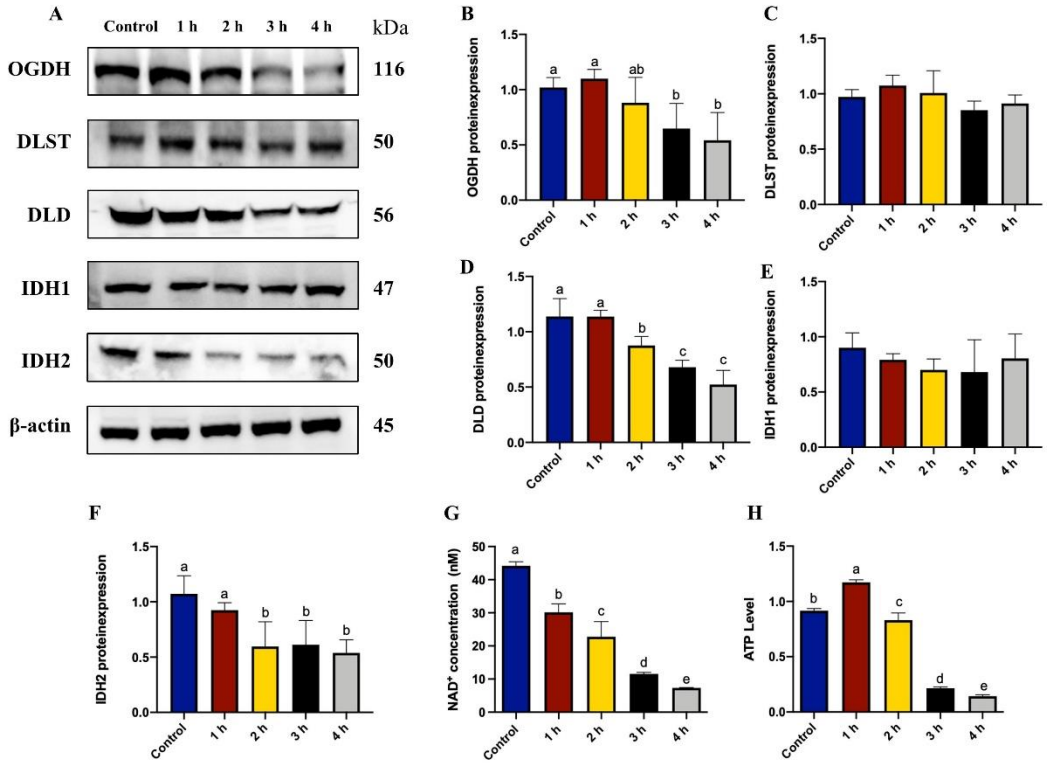

Fig. 6 Changes in expression levels of expression levels of key enzymes in the tricarboxylic acid cycle as well as NAD^+ and ATP following Zn treatment. Alterations in protein expression levels of cytoplasmic oxidative stress-related proteins at various time intervals following Zn overload, including OGDH, DLST, DLD, IDH1, and IDH2 (A-F). Results are given as mean ± SD (n=3-5). Changes in NAD^+ levels after Zn supplementation (G). Changes in ATP levels following Zn treatment (H). Results are given as mean ± SD (n=8). Groups labeled without a common letter were significantly different (P<0.05).

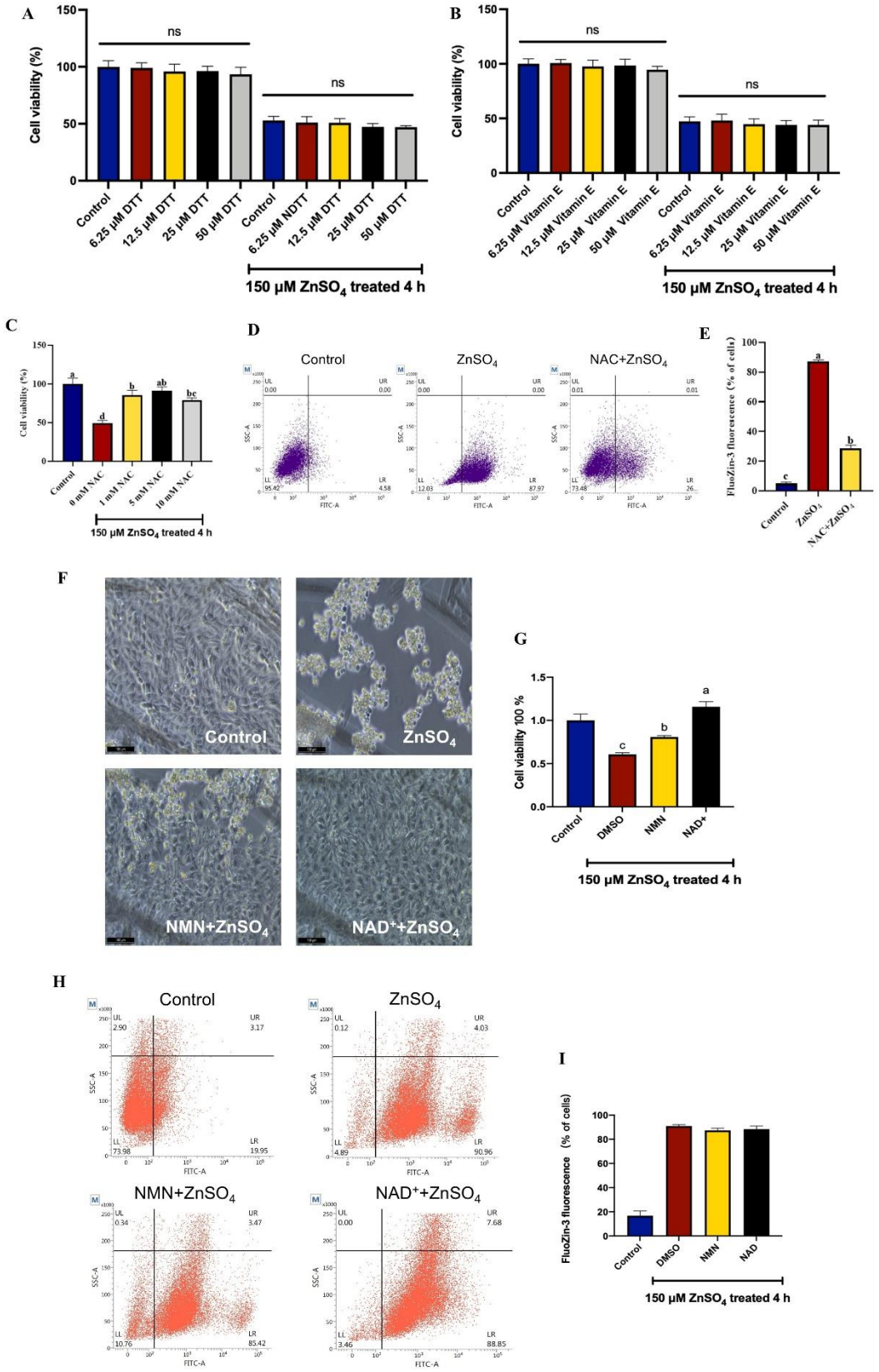

Fig. 7 The alleviating effect of NAD^+ supplementation on Zn overload-induced cell death. Effects of antioxidants DTT (A), Vitamin E (B) and NAC (C) on Zn overload-induced cytotoxicity (n=6). Flow

cytometric analysis of intracellular Zn^{2+} (D). Quantification of intracellular Zn^{2+} levels (E) (n=3). Microscopy imaging (F). The influence of NAD^+ supplementation on cell viability in high Zn concentrations, with NMN and NAD^+ added at a concentration of 1 mM (G) (n=6). Flow cytometric analysis of intracellular Zn^{2+} (H). Quantification of intracellular Zn^{2+} levels (I) (n=3). Results are given as mean ± SD; groups labeled without a common letter were significantly different (P<0.05).

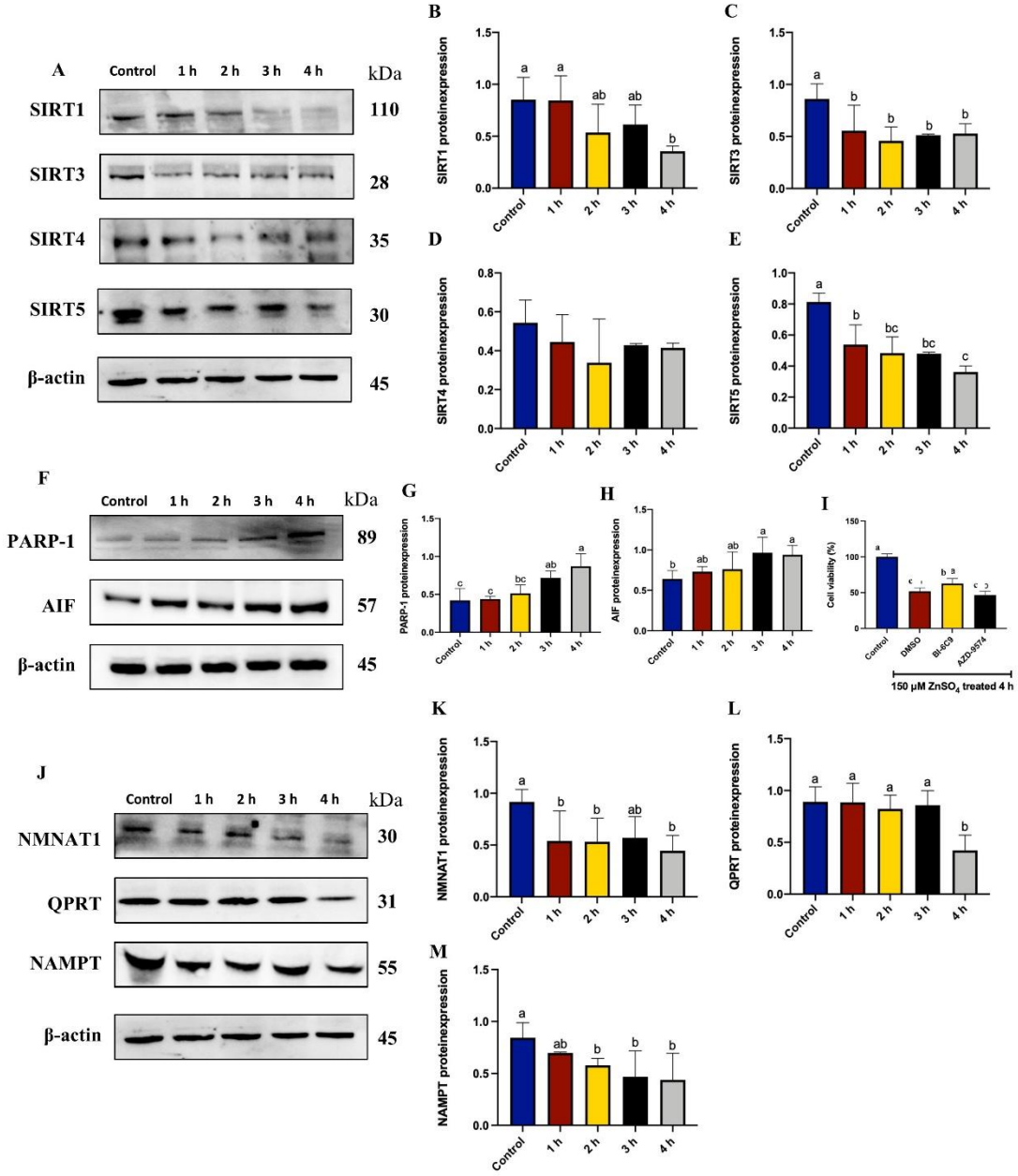

Fig. 8 Changes in expression levels of NAD^+-dependent Sirtuin protein family, PARP-1 pathway proteins and NAD^+ synthesis enzymes following Zn treatment. Alterations in protein expression levels of cytoplasmic oxidative stress-related proteins at various time intervals following Zn overload, including SIRT1, SIRT3, SIRT4, and SIRT5 (A-E) (n=3-5). Alterations in protein expression levels of PARP-1-related proteins at various time intervals following Zn overload, including PARP-1, and AIF (F-H) (n=3-5). (I) The alleviating impact of AIF inhibitor (BI-6C9, 5μM) and PARP-1 inhibitor (AZD-9574, 5μM) (n=6).

Alterations in protein expression levels of NAD^+ synthesis enzymes at various time intervals following Zn overload, including NMNAT1, QPRT, and NAMPT (J-M) (n=3-5). Results are given as mean ± SD. Groups labeled without a common letter were significantly different (P<0.05).

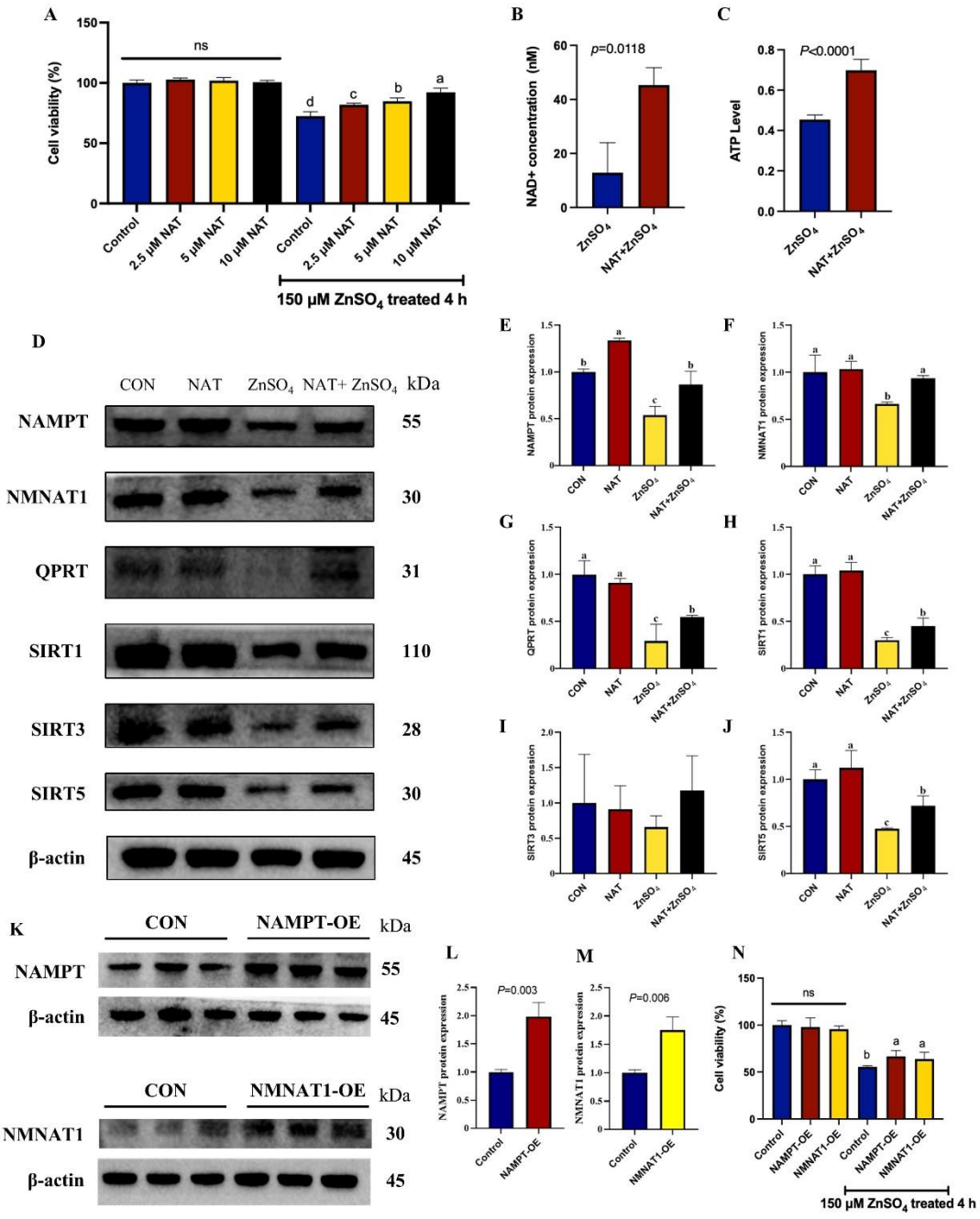

Fig. 9 The alleviating effect of boosting NAD^+ synthesis on Zn overload-induced cell death. The alleviating impact of NAMPT activator NAT on cell viability (A) (n=6), NAD^+ concentration (B), ATP level (C) (n=4), and the protein expression of NAMPT, NMNAT1, QPRT, SIRT1, SIRT3 as well as SIRT5 (D-J) (n=3). The over expression efficiency of NMNAT1 and NAMPT (K-M) (n=3). The alleviating impact of NMNAT1 and NAMPT overexpression (N) (n=6). Statistical significance on the effects of NAT on protein expressions was determined using one-way ANOVA, followed by Duncan test. Results are given as mean ± SD; groups labeled without a common letter were significantly different (P<0.05).

Graphical abstract